

Modeling of a voltammetric experiment in a limiting diffusion space

Valentin Mirčeski · Živorad Tomovski

Received: 1 March 2010 / Revised: 24 April 2010 / Accepted: 26 April 2010 / Published online: 20 May 2010
© Springer-Verlag 2010

Abstract A voltammetric experiment confined in a limiting diffusion space is analyzed theoretically governed by conventional or time-anomalous fractional diffusion under conditions of cyclic and square-wave voltammetry. The solution for conventional diffusion is derived by means of the Jacobi theta function $\Theta(a^2/\pi^2 t)$ ($a = LD^{-1/2}$, where L is the thickness of the finite diffusion space, D is the diffusion coefficient, and t is the time of the experiment) and compared with the solution frequently used in the literature expressed in the form $\Theta(a^{-2}t)$. For $L \rightarrow \infty$, the present solution converges to the one for the semi-infinite diffusion, thus being of a general applicability for both finite and semi-infinite diffusion. Hence, the mathematical model for simulation of both cyclic and square-wave voltammetric experiment provides significant advances in terms of simulation time and accuracy compared to the previous model based on the modified step-function method Mirčeski (J Phys Chem B 108:13719, 2004). For the fractional diffusion experiment, the solution is derived by combining an infinite series and the Wright function $\varphi(-\alpha/2, \alpha/2; -2a\xi^{-1/2}t^{-\alpha/2})$, where α is the time fractional parameter ranging over the interval $0 < \alpha < 1$, and $\xi = 1 \text{ s}^{1-\alpha}$ is the auxiliary constant. The voltammetric properties of the experiment controlled by fractional diffusion are comparable for both finite and semi-infinite diffusion.

Keywords Mathematical modeling · Voltammetry · Limiting diffusion · Thin film · Fractional diffusion

Introduction

Electrochemical processes confined in a restricted diffusion space are subject of a permanent interest in the electrochemical science since the early 1960s of the last century when the thin-layer electrochemical cells were first developed [1, 2]. Later on, the efforts to study such processes were permanently increasing following the advances of the chemically modified electrodes [3–5], where the electroactive species are, in most of the cases, confined within a thin film immobilized on the electrode surface. It is well known that the electrochemical properties of an electrode modified with an electroactive layer depend significantly on the layer thickness. When the electroactive material is present in a form of a sub-monomolecular layer the electrode reaction proceeds as a surface process, making the mathematical modeling rather simple as the mass transfer phenomena have not to be considered [6]. The theory for surface electrode processes is well developed, being a basis for understanding many advanced applications of electrochemical techniques, such as functioning of electrochemical sensors [7], processes in protein film voltammetry [8], self-assembled monolayers, etc. In the case of thicker films, e.g., polymer-modified electrodes [9], the mass transfer within the interior of the film needs to be addressed, which is a challenging task when the thickness of the film is lower than the diffusion layer. Such cases are also encountered during anodic stripping voltammetry at mercury [10, 11], bismuth [12], antimony [13] film electrodes, electrodes modified with solid microparticles, and droplets [14], (i.e., three-phase electrodes), thin-

V. Mirčeski (✉)
Institute of Chemistry, Faculty of Natural Sciences
and Mathematics, “Ss Cyril and Methodius” University,
P.O. Box 162, 1000 Skopje, Republic of Macedonia
e-mail: valentin@pmf.ukim.mk

Ž. Tomovski
Institute of Mathematics, Faculty of Natural Sciences
and Mathematics, “Ss Cyril and Methodius” University,
P.O. Box 162, 1000 Skopje, Republic of Macedonia

organic-film electrodes [15, 16], etc., pointing out they are still in the focus of the contemporary electroanalytical science.

It is worth mentioning here that in the last decade, the application of square-wave voltammetry (SWV) [17] to three-phase and thin-organic-film modified electrodes resulted in significant advances in the electrochemistry at liquid interfaces, in particular related with both ion [18–21] and electron [22] transfer reactions. For these reasons, the modeling of a SW voltammetric experiment governed by a finite diffusion is becoming an increasingly important subject. Recently, an attempt has been made to address theoretically a thin film experiment of a kinetically controlled electrode reaction under conditions of SWV applying modified step-function method [23, 24]. The theory for a reversible electrode reaction in a thin-layer cell for SWV has been initially developed by Aoki and Osteryoung [25], which relays on previous theories of linear sweep voltammetry [26–29].

In the present communication, we continue our work on modeling voltammetry under limiting diffusion space considering both cyclic (CV) and square-wave voltammetry. We attempt to provide theoretical background for wide experimental conditions; therefore, we address both conventional and fractional diffusion mass transfer [30–32], the latter being particularly important for electrodes modified with solid films. Recently, we initiated the study of a fractional semi-infinite diffusion [33], which is here extended to the experiment restricted in a limiting diffusion space.

Mathematical model

Conventional diffusion

A simple electrode reaction of two chemically stable species Ox and Red characterized with a common diffusion coefficient D , embedded in a thin film of a thickness L , is considered:



For the sake of simplicity, the charge of the species is omitted. At the beginning of the experiment, only Red form is homogeneously distributed in the film at concentration $c_{\text{Red}}(x, 0) = c^*$. Thus, considering a conventional diffusion, the boundary value problem for the Ox species is represented by the following model:

$$\frac{\partial c_{\text{Ox}}(x, t)}{\partial t} = D \frac{\partial^2 c_{\text{Ox}}(x, t)}{\partial x^2} \quad (1)$$

$$t = 0, 0 \leq x \leq L : c_{\text{ox}}(x, 0) = 0 \quad (2)$$

$$t > 0, x = 0 : \frac{\partial c_{\text{ox}}(0, t)}{\partial x} = -\frac{I(t)}{nFAD} \quad (3)$$

$$t > 0, x = L : -D \frac{\partial c_{\text{ox}}(L, t)}{\partial x} = 0 \quad (4)$$

Applying Laplace transforms to (1) one gets:

$$\begin{aligned} \bar{c}_{\text{Ox}}(x, s) &= A(s) \exp\left[-\left(x/\sqrt{D}\right)s^{1/2}\right] + B(s) \\ &\times \exp\left[\left(x/\sqrt{D}\right)s^{1/2}\right] \end{aligned} \quad (5)$$

$$\begin{aligned} \frac{\partial \bar{c}_{\text{Ox}}(x, s)}{\partial x} &= -\frac{A(s)s^{1/2}}{\sqrt{D}} \exp\left[-\left(x/\sqrt{D}\right)s^{1/2}\right] \\ &+ \frac{B(s)s^{1/2}}{\sqrt{D}} \exp\left[\left(x/\sqrt{D}\right)s^{1/2}\right] \end{aligned} \quad (6)$$

From the conditions (3) and (4) follows:

$$-\frac{A(s)s^{1/2}}{\sqrt{D}} + \frac{B(s)s^{1/2}}{\sqrt{D}} = -\frac{\bar{I}(s)}{nFAD} \quad (7)$$

$$\begin{aligned} -\frac{A(s)s^{1/2}}{\sqrt{D}} \exp\left[-\left(L/\sqrt{D}\right)s^{1/2}\right] &+ \frac{B(s)s^{1/2}}{\sqrt{D}} \\ &\times \exp\left[\left(L/\sqrt{D}\right)s^{1/2}\right] \\ &= 0 \end{aligned} \quad (8)$$

The system of Eqs. 7, 8 can be solved to find the constants $A(s)$ and $B(s)$ as follows:

$$A(s) = \frac{\bar{I}(s)}{nFA\sqrt{D}} s^{-1/2} \frac{\exp[2(L/\sqrt{D})s^{1/2}]}{\exp[2(L/\sqrt{D})s^{1/2}] - 1} \quad (9)$$

$$B(s) = \frac{\bar{I}(s)}{nFA\sqrt{D}} s^{-1/2} \frac{1}{\exp[2(L/\sqrt{D})s^{1/2}] - 1}. \quad (10)$$

Substituting (9–10) into (5) yields:

$$\bar{c}_{\text{Ox}}(x, s) = \frac{\bar{I}(s)}{nFA\sqrt{D}} s^{-1/2} \frac{\left[\exp((L-x)/\sqrt{D})s^{1/2}\right] + \left[\exp(-(L-x)/\sqrt{D})s^{1/2}\right]}{\exp[(L/\sqrt{D})s^{1/2}] - \exp[-(L/\sqrt{D})s^{1/2}]} \quad (11)$$

As we are primarily interested for the solution at the electrode surface, i.e., $x=0$, Eq. 11 simplifies to the following form:

$$\bar{c}_{\text{Ox}}(0, s) = \frac{\bar{I}(s)}{nFA\sqrt{D}} s^{-1/2} \frac{\exp(as^{1/2}) + \exp(-as^{1/2})}{\exp(as^{1/2}) - \exp(-as^{1/2})}, \quad (12)$$

where $a = L/\sqrt{D}$. Taking advantage of the hyperbolic function $\coth(x) = \frac{\exp(x)+\exp(-x)}{\exp(x)-\exp(-x)}$, Eq. 12 is rewritten as:

$$\overline{c_{\text{Ox}}}(0, s) = \frac{\overline{I(s)}}{nFA\sqrt{D}} s^{-1/2} \coth(as^{1/2}). \quad (13)$$

The inverse Laplace transform of (13) is:

$$c_{\text{Ox}}(0, t) = \frac{1}{anFA\sqrt{D}} \int_0^t I(\tau) \Theta[(t-\tau)a^{-2}] d\tau, \quad (14)$$

where $\Theta(t)$ is the Jacobi theta function defined as

$$\Theta(t) = \Theta(0, t) = 1 + 2 \sum_{k=1}^{\infty} \exp(-\pi^2 tk^2). \quad (15)$$

The function (15) is a special case of the Jacobi theta function of two variables [34]

$$\Theta(x, t) = 1 + 2 \sum_{k=1}^{\infty} \exp(-\pi^2 tk^2) \cos(2\pi kx) \quad (16)$$

(for $x=0$), which is the unique solution to the one-dimensional heat equation with periodic boundary conditions at time zero. The type of solution (14) has been frequently used in the previous theoretical works [25, 28, 29].

Alternatively, a new solution can be inferred by taking advantage of the following expansion:

$$\frac{1}{e^x - e^{-x}} = \frac{e^{-x}}{1 - e^{-2x}} = e^{-x} \sum_{k=0}^{\infty} e^{-2kx} = \sum_{k=0}^{\infty} e^{-(2k+1)x} \quad (17)$$

which is valid for all $x \in \mathbf{R}$. Hence, Eq. 12 can be transformed into the following series:

$$\begin{aligned} \overline{c_{\text{Ox}}}(0, s) &= \frac{\overline{I(s)}}{nFA\sqrt{D}} s^{-1/2} \left\{ \sum_{k=0}^{\infty} \exp(-2kas^{1/2}) + \sum_{k=0}^{\infty} \exp[-(2k+2)as^{1/2}] \right\} \\ &= \frac{\overline{I(s)}}{nFA\sqrt{D}} s^{-1/2} \left\{ 1 + 2 \sum_{k=1}^{\infty} \exp(-2kas^{1/2}) \right\}. \end{aligned} \quad (18)$$

By convolution theorem the inverse Laplace transform reads:

$$\begin{aligned} c_{\text{Ox}}(0, t) &= \frac{1}{nFA\sqrt{D}} \int_0^t \frac{I(\tau)}{\sqrt{\pi(t-\tau)}} \left\{ 1 + 2 \sum_{k=1}^{\infty} \exp\left(-\frac{a^2 k^2}{t-\tau}\right) \right\} d\tau \\ &= \frac{1}{nFA\sqrt{D}} \int_0^t \frac{I(\tau)}{\sqrt{\pi(t-\tau)}} \Theta\left(\frac{a^2}{\pi^2(t-\tau)}\right) d\tau. \end{aligned} \quad (19)$$

Fractional diffusion

The subject of fractional calculus has gained importance and popularity during the past three decades, due mainly to the

applicability in numerous seemingly diverse fields, such as electromagnetism, control engineering, fractional viscoelastic models, diffusion theory, continuum mechanics, signal processing, electrochemistry, etc. Indeed, it provides several useful tools for solving differential, integral and integro-differential equations, and a variety of problems involving special functions of mathematical physics as well as their extensions and generalizations in one and more variables.

There are several definitions leading to different results, making difficult to establish a general theory of fractional calculus. The Riemann–Liouville is one of the known definitions. The (R–L) integral operator \mathfrak{I}^α of order $\alpha (\alpha \in \mathbf{C})$ is defined by (see Chapter 13 in Erdelyi et al. [35])

$$(\mathfrak{I}^\alpha f)(x) = \frac{1}{\Gamma(\alpha)} \int_0^x (x-t)^{\alpha-1} f(t) dt \quad (\Re(\alpha) > 0) \quad (20)$$

where $\Gamma(\alpha) = \int_0^\infty t^{\alpha-1} e^{-t} dt$ is the Gamma function.

The operator $D_{t;0}^\alpha$ of fractional derivative of order $\alpha (\alpha \in \mathbf{C})$ which corresponds to the fractional integral operator \mathfrak{I}^α is defined as

$$(D_{t;0}^\alpha f)(t) = \frac{d^m}{dt^m} (\mathfrak{I}^{m-\alpha} f)(t) \quad (m-1 \leq \Re(\alpha) \leq m; m \in \mathbf{N}). \quad (21)$$

The Laplace transform of $D_{t;0}^\alpha$ is given by the formula:

$$\begin{aligned} L\left\{ (D_{t;0}^\alpha f)(t) : s \right\} &= s^\alpha F(s) - \sum_{k=0}^{n-1} s^k (D_{t;0}^{\alpha-k-1} f(t))|_{t=0} \\ &\quad (n-1 \leq \Re(\alpha) \leq n; n \in \mathbf{N}) \end{aligned} \quad (22)$$

where

$$L\{f(t) : s\} = \int_0^\infty e^{-st} f(t) dt = F(s) \quad (23)$$

provided that the integral exists.

Anomalous diffusion in the presence or absence of an external velocity or force field has been modeled in numerous ways. Mathematical aspects of the boundary-value problems in physics have been treated in the works of Engler [36], Fujuta [37], Gorenflo et al. [38], Mainardi et al. [39–41], Prüss [42], Podlubny [43], Schneider and Wyss [44], Wyss [45], Hilfer [46], etc. In the recent work [33], a cyclic voltammetric experiment governed by anomalous semi-infinite diffusion of an electroactive species is analyzed by means of fractional calculus.

If nonconventional diffusion has to be considered of a fractional order $\alpha (0 < \alpha < 1)$ with respect to the time variable, the following fractional differential equation of order α has to be solved

$$\frac{\partial^\alpha c_{\text{Ox}}(x, t)}{\partial t^\alpha} = D\xi \frac{\partial^2 c_{\text{Ox}}(x, t)}{\partial x^2}, \quad (24)$$

under conditions (2)–(4), where $\xi=1$ s $^{1-\alpha}$ is an auxiliary constant to account for the dimensionless correctness of Eq. 24. Applying Laplace transforms to (24) and following similar procedure as in the previous section, the solution in a Laplace domain is:

$$\overline{c_{\text{Ox}}}(0, s) \approx \frac{\overline{I(s)}}{nFA\sqrt{D/\xi}} s^{-\alpha/2} \left\{ 1 + 2 \sum_{k=1}^3 \exp\left(-2ka\xi^{-1/2}s^{\alpha/2}\right) \right\}. \quad (25)$$

To derive the later solution, the following property has been used: $\frac{1}{1-q} = 1 + q + q^2 + o(q^2)$ ($0 < q < 1$) for $q = e^{-2x}$. Thus, from (17), it follows

$$\frac{1}{e^x - e^{-x}} = e^{-x} + e^{-3x} + e^{-5x} + o(e^{-5x}).$$

Since

$$\begin{aligned} L\left(t^{\frac{\alpha}{2}-1} \varphi\left(-\frac{\alpha}{2}, \frac{\alpha}{2}; -2ka\xi^{-1/2}t^{-\alpha/2}\right)\right) \\ = s^{-\alpha/2} e^{-2ka\xi^{-1/2}s^{\alpha/2}} \end{aligned} \quad (26)$$

the inverse Laplace transform of (25) reads:

$$\begin{aligned} c(0, t) \approx \int_0^t \frac{\overline{I(\tau)}}{nFA\sqrt{D/\xi}} (t-\tau)^{\alpha/2-1} \\ \left(1 + 2 \sum_{k=1}^3 \varphi\left(-\frac{\alpha}{2}, \frac{\alpha}{2}; -2ka\xi^{-1/2}(t-\tau)^{-\alpha/2}\right) \right) d\tau \end{aligned} \quad (27)$$

Here, $\varphi(\alpha, \beta; z)$ is the Wright function [35] defined as

$$\varphi(\alpha, \beta; z) = \sum_{k=0}^{\infty} \frac{1}{\Gamma(\alpha k + \beta)} \frac{z^k}{k!} \quad (\Re(\alpha), \Re(\beta) > -1) \quad (28)$$

According to the mass preservation law for the electrode reaction, the following condition is valid: $c_{\text{Red}}(0, t) + c_{\text{Ox}}(0, t) = c^*$. Hence, the solution for $c_{\text{Red}}(0, t)$ is obvious for both conventional and fractional diffusion. If the electrode reaction is reversible the solutions for $c_{\text{Red}}(0, t)$ and $c_{\text{Ox}}(0, t)$ has to be combined with the Nernst equation $c_{\text{Ox}}(0, t) = c_{\text{Red}}(0, t) \exp(\phi)$, where $\phi = \frac{nF}{RT} (E - E_c^\circ)$ is dimensionless electrode potential measured versus the formal potential E_c° of reaction (I). Otherwise, if the electrode reaction is kinetically controlled, characterized with a standard rate constant k_s and electron transfer coefficient β , the current–potential relationship can be predicted on the basis of Butler–Volmer kinetic equation: $\frac{I}{nFA} = k_s \exp(\beta\phi) [c_{\text{Red}}(0, t) - \exp(-\phi)c_{\text{Ox}}(0, t)]$. For practical purposes, in order to predict the outcome of the voltammetric experiment, it is convenient to apply the step-function method [47] to derive

a recurrent formula for simulation of the experiment. For a conventional cyclic voltammetry, the recurrent formula is:

$$\Psi_m = \frac{\frac{\exp(\phi_m)}{[1+\exp(\phi_m)]\sqrt{\theta}} - \sum_{j=1}^{m-1} \Psi_m S_{m-j+1}}{S_1}. \quad (29)$$

For derivation of Eq. 29, the total time of the voltammetric experiment was incremented, where m is the serial number of time increments. The time increment was defined as $d = \frac{\Delta E}{v}$, where ΔE (V) is the step potential, and v is the sweep rate (V s $^{-1}$). In this study, the step potential was set to 0.1 mV. In addition, $\theta = \frac{nF}{RT} v$ and $\Psi = \frac{I}{nFAc^*} \sqrt{D\theta}$ is dimensionless current function factor, depends which solution will be taken. Following Eq. 14, one gets:

$$S_m = \frac{1}{a} \left(d + \frac{2a^2}{\pi} \sum_{k=1}^{\infty} \frac{e^{-\pi k^2 a^{-2}(m-1)d} - e^{-\pi k^2 a^{-2}md}}{k^2} \right). \quad (30)$$

Following Eq. 19, the numerical integration factor is defined as follows:

$$S_m = \int_{(m-1)d}^{md} \frac{1}{\sqrt{\pi t}} dt + 2 \sum_{k=1}^{\infty} \int_{(m-1)d}^{md} \frac{\exp\left(\frac{-a^2 k^2}{t}\right)}{\sqrt{\pi t}} dt \quad (31)$$

We note that the type of integral arising in (31) has the following solution

$$\begin{aligned} \int \frac{\exp(-z/t)}{\sqrt{t}} dt &= 2\sqrt{t} \exp(-z/t) + 2 \\ &\times \sqrt{z\pi} \operatorname{erf}\left(\sqrt{z/t}\right) + C. \end{aligned} \quad (32)$$

To simulate the experiment under conditions of advanced square-wave voltammetry, the same numerical solution (29) can be applied, replacing the parameter θ with the frequency of the potential modulation f and defining the time increment as $d = \frac{1}{50f}$. Accordingly, the dimensionless current function is defined as $\Psi = \frac{I}{nFAc^*} \sqrt{Df}$

For the voltammetric experiment governed by a fractional diffusion the numerical integration factor is defined as

$$S_m = \int_{(m-1)d}^{md} t^{\alpha/2-1} \left[1 + 2 \sum_{k=1}^3 \varphi\left(-\frac{\alpha}{2}, \frac{\alpha}{2}; -2ka\xi^{-1/2}t^{-\alpha/2}\right) \right] dt. \quad (33)$$

Results and discussion

For a conventional diffusion and a reversible electrode reaction, the voltammetric response is predominantly

controlled by the thickness parameter defined as $\Lambda = L\sqrt{\frac{v}{D}}$ and $\Lambda = L\sqrt{\frac{f}{D}}$ for cyclic and SW voltammetry, respectively, which unifies the thickness of the film, time-window of the voltammetric experiment, and rate of diffusion. The influence of the thickness parameter to the voltammetric response is well known for both techniques [24, 25, 28, 29]. Figure 1 compares the dimensionless cyclic and SW voltammograms simulated on the basis of Eqs. 14 and 19. Two cyclic voltammograms are almost identical in a qualitative sense, whereas the deviation for the SW voltammograms is slightly more pronounced. The simulations for both techniques are performed for identical film thickness and diffusion coefficient, the main difference being in the characteristic time-window of the experiment, i.e., $v=100$ mV/s for CV, and $f=50$ s⁻¹ for SWV. The relative average difference in calculating the two net SW voltammograms is 2.83%, whereas for cyclic voltammograms, it is 1.96%. Differences are not constant for all conditions of the simulations, revealing that the two solutions do not lead to the same result. However, the discrepancy cannot be even improved by decreasing the time increment used for the simulations, e.g., from $d=1/50f$ to $d=1/100f$ or $d=1/200f$. This indicates that the differences originate from the different underlying mathematics represented by the formula (14) and (19), rather than from the error involved by the general step-function method [47] used to derive the numerical formula (29).

Using a mathematical solution that relies on an infinite series, the reliability of the results critically depends on the convergence property of the series used; hence, this feature has to be carefully considered using numerical simulations. Generally, the convergence depends on the film thickness, time of the voltammetric experiment, and the diffusion coefficient. Numerical simulations reveal that the Jacobi theta function $\Theta(ta^{-2})$ used in the solution (14) is more appropriate for low film thicknesses, while the contrary holds for the theta function $\Theta(\frac{a^2}{\pi^2 t})$ arising in the solution (19). For illustration, the convergence has been checked by assuming time of $t=5$ s and diffusion coefficient of $D = 5 \times 10^{-6}$ cm²s⁻¹, as typical for a conventional voltammetric experiment. For $1 \leq L/\mu\text{m} \leq 100$ and $100 < L/\mu\text{m} \leq 1000$ the function $\Theta(ta^{-2})$ converges after the third and 25th series element, respectively. For $L=3000$ μm the convergence commences after the 74th element, and for larger L , the function is inappropriate for simulations of the experiment. On the contrary, the theta function $\Theta(\frac{a^2}{\pi^2 t})$ converges after the 170th and 84th series element for $L=1$ and 2 μm , respectively; for $3 \leq L/\mu\text{m} \leq 10$ and $10 < L/\mu\text{m} \leq 100$, the convergence is reached after the 54th and 15th element, respectively, and for $L>100$ μm , the convergence is

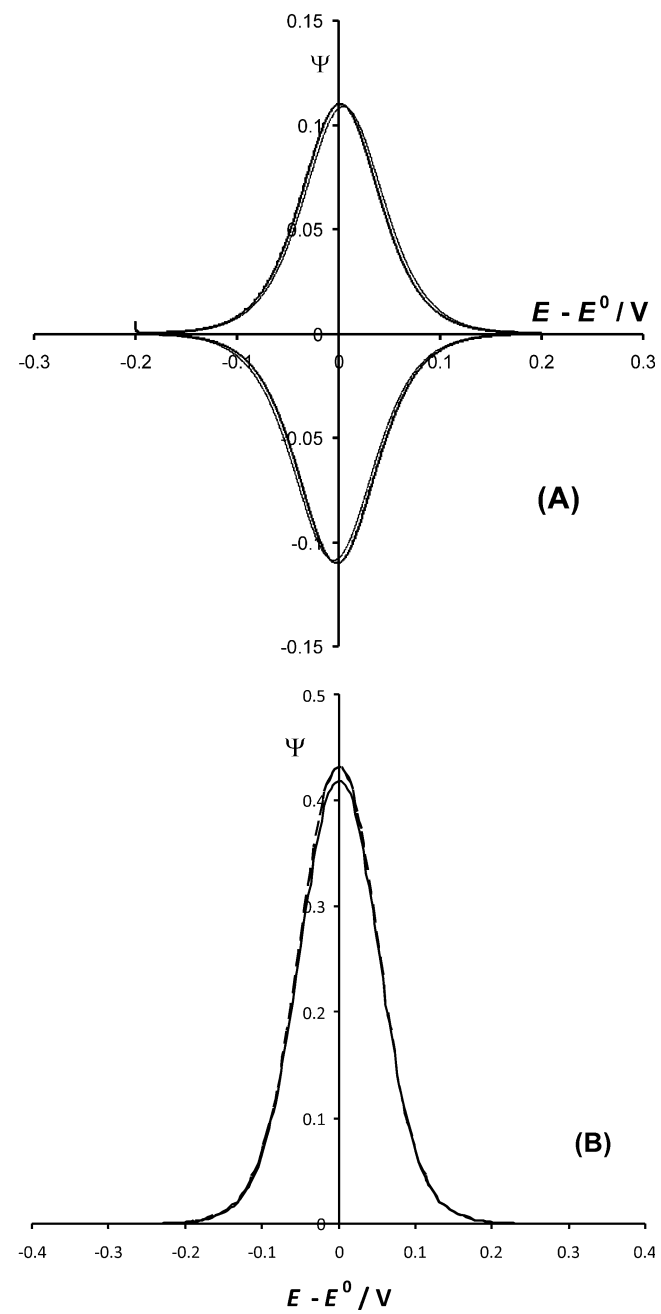


Fig. 1 Comparison of cyclic (a) and SW (b) voltammograms for a reversible electrode reaction simulated using numerical integration factor given in Eq. 14 (dashed line) and Eq. 19 (full line). Conditions of the simulations are: number of elements in the series $N=100$, film thickness $L=5$ μm and diffusion coefficient, $D = 5 \times 10^{-6}$ cm²s⁻¹. In addition, for CV, the sweep rate is $v=100$ mV/s and scan increment $\Delta E=0.1$ mV. For SWV, the frequency is $f=50$ Hz, amplitude $E_{sw}=50$ mV, and step potential increment $\Delta E=5$ mV

achieved after the 1st element. In addition, the latter function has another very important feature. Namely, for $L \rightarrow \infty$, the limiting value is 1, i.e., $\lim_{a \rightarrow \infty} \Theta(\frac{a^2}{\pi^2 t}) = 1$ (recall that $a = L/\sqrt{D}$). Hence, for $L \rightarrow \infty$, the solution (19)

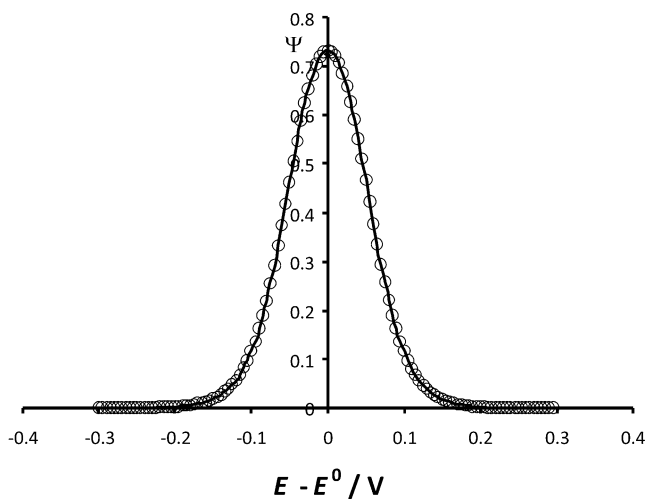


Fig. 2 Comparison of the simulated net SW voltammograms for a reversible electrode reaction in a thin film of thickness $L=0.01$ cm (solid line) based on the solution given by Eq. 19 and for semi-infinite diffusion (cycles) Eq. 34. Conditions of the simulations are the same as for Fig. 1

simplifies to the well-known solution for a semi-infinite case [48]:

$$\begin{aligned} c_{Ox}(0, t) &= \frac{1}{nFA\sqrt{D}} \int_0^t \frac{I(\tau)}{\sqrt{\pi(t-\tau)}} d\tau \\ &= \frac{1}{nFA\sqrt{D}} \Im^{1/2} I(t). \end{aligned} \quad (34)$$

This reveals that the solution (19) is of general importance, being capable to describe an electrochemical

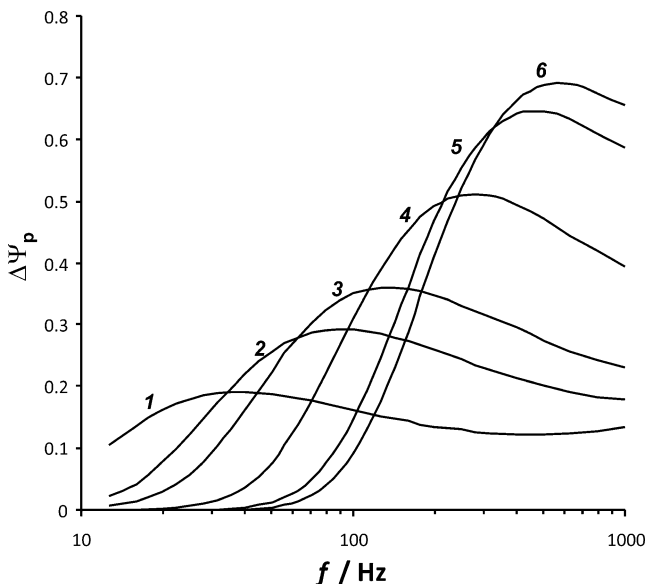


Fig. 3 Quasireversible maximum in thin film SWV. The standard rate constant is $k_s = 2 \times 10^{-3}$ (1); 5×10^{-3} (2); 8×10^{-3} (3); 2×10^{-2} (4); 5×10^{-2} (5), and 8×10^{-2} cm s^{-1} (6). The film thickness is $L=1$ μm , and the other conditions are the same as for Fig. 1

experiment under both limiting and semi-infinite diffusion conditions. Figure 2 confirms the latter property by comparing the net SW voltammograms simulated with the aid of Eq. 19 (for $L=0.01$ cm) and Eq. 34 valid for the semi-infinite diffusion. The two voltammograms are practically identical.

Besides the reversible case, it is useful to demonstrate the capability of the solution (19) to simulate the quasireversible electrode reaction in a thin film. For illustration, the feature of quasireversible maximum in SWV is selected, as it has been extensively exploited for estimation of important kinetic parameters in previous studies [21, 49, 50]. Figure 3 depicts well-developed quasireversible maxima, plotted by analyzing the variation of the dimensionless net SW peak current as a function of the modulation frequency. This type of simulations is analogous to the measurement of the quasireversible

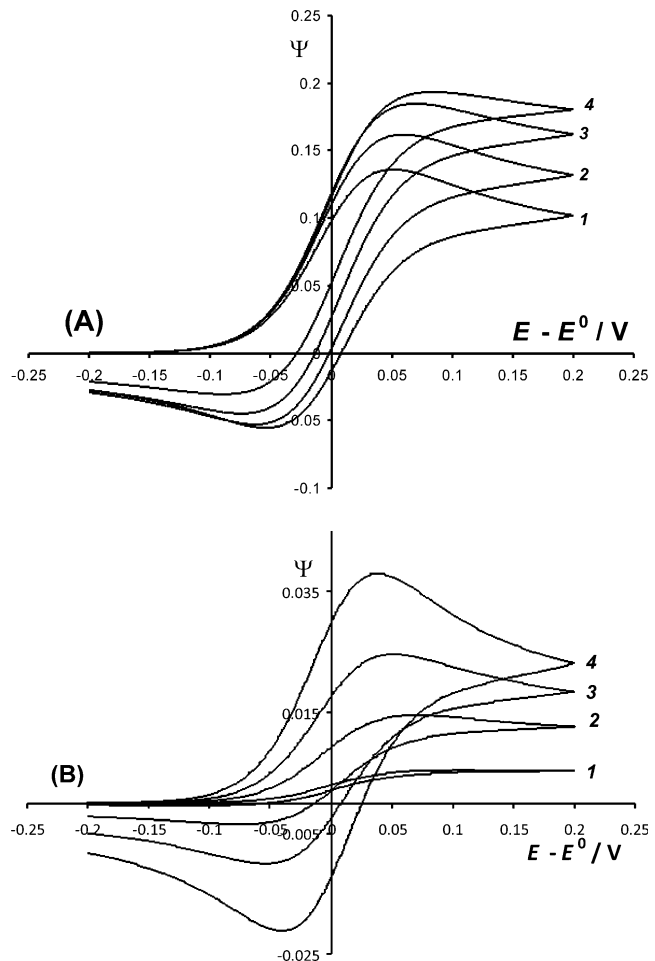


Fig. 4 Typical cyclic voltammograms for fractional diffusion in a thin film. The values of the fractional parameter $\alpha=0.55$ (1), 0.44 (2), 0.33 (3), and 0.22 (4) for (a); $\alpha=0.11$ (1), 0.33 (2), 0.55 (3), and 0.77 (4) for (b). The conditions of the simulations are: sweep rate $v=1$ mV/s (a) and 2 V/s (b), thin film thickness $L=0.05$ μm , number of elements in the series $N=3$, number of elements in the Gamma function $K=100$, and diffusion coefficient $D=5 \times 10^{-6}$ cm^2s^{-1}

maxima in the experimental studies [21, 49, 50]. The evolution of the maxima simulated for different standard rate constants clearly shows the maximum position is proportional to the value of the standard rate constant, enabling estimation of the latter parameter in a simple procedure, as already theoretically described [24] and experimentally confirmed [21, 49, 50]. It is finally important to stress that the current model provides significant improvements of the overall procedure for kinetic measurements in terms of the precision of the simulated results and the time of numerical simulations compared to the previous procedure described in [23, 24].

Finally, we discuss briefly the outcome of the simulations for fractional diffusion. The main features of the voltammetry, governed by a fractional, time-anomalous mass transport, have been recently elaborated for a semi-infinite case [33]. When the fractional parameter α decreases from 1 to 0, the cyclic voltammograms transform in the shape and magnitude, commonly altering from a wave-like to a sigmoid-like I - E curve. For a low α , the concentration gradient is virtually constant in the course of the voltammetric experiment causing a steady-state-like voltammetric behavior and a sigmoid shape of the voltammetric curves [33].

In the present study, the solution for a fractional diffusion is given by Eq. 27, which is only an approximation, as it is based on a divergent series. For calculations, only the first three terms of the series are taken into account. Nevertheless, the present model can provide qualitative information on the expected voltammetric behavior for a thin-film experiment governed by a fractional diffusion. Figure 4 shows the evolution of cyclic voltammograms with the fractional parameter α , for a reversible electrode reaction confined in a film of thickness $L=0.05\text{ }\mu\text{m}$. Two sets of simulations have been conducted referring to slow ($v=1\text{ mV/s}$) and fast ($v=2\text{ V/s}$) sweep rate. Regardless the sweep rate, the voltammograms deviate strongly from the common peak-like shaped voltammograms observed in a thin film with a conventional mass transfer (e.g., Fig. 1). Hence, with anomalous diffusion, which is attributed with almost a constant concentration gradient in the course of the experiment [33], the exhaustion of the film is unlikely to be achieved, making the overall voltammetric behavior similar as in the case of semi-infinite fractional diffusion. When the electrolysis time is long (Fig. 4A), the magnitude of the voltammograms decreases by increasing α , while the effect is opposite for a short electrolysis time (Fig. 4b). This is a consequence of the specific chronoamperometric characteristics of the fractional voltammetric experiment (see Eq. 34 in [33]). Namely, for the fractional diffusion the current is proportional to $t^{-\alpha/2}$. For a short electrolysis time (fast sweep rate) the current is larger for larger α . However, at

longer electrolysis time (slow sweep rate), the current decreases more severely for larger α , causing the magnitude of the response to decrease by increasing α .

Conclusion

The classical problem of a voltammetric experiment confined in a restricted diffusion space is addressed theoretically for both conventional and fractional time-anomalous diffusion. To the best of our knowledge, new mathematical solutions are derived for both cases. The solution given by Eq. 19, referring to a conventional diffusion, is of general importance, as it is capable to predict the outcome of the voltammetric experiment governed by the diffusion of electroactive species in both restricted and semi-infinite diffusion conditions. The model presented here is significantly improved in terms of accuracy and simulation time compared to the previous one based on the modified step-function method [23, 24]. For the complex experiment affected by limited and fractional time-anomalous diffusion, an approximate solution is derived only Eq. 27 that involves a divergent series. Nevertheless, the solution is capable to predict qualitatively the main features of the voltammetric experiment.

References

- Christensen CR, Anson FC (1963) Anal Chem 35:205
- Hubbard AT, Anson FC (1970) Electroanal Chem 4:129
- Chidsey CED, Murray RW (1986) Science 231:25
- Murray RW, Ewing AG, Durst RA (1987) Anal Chem 59:379A
- Fujihira M, Rubinstein I, Rusling JF (2007) Modified Electrodes. In: Bard AJ, Stratmann M (eds) Encyclopedia of Electrochemistry, vol 10. Wiley, Weinheim
- Laviron E (1967) Bull Soc Chim France 1967:3717
- Schelfer F, Schubert F (eds) (1992) Biosensors: techniques and instrumentation in analytical chemistry, vol 11. Elsevier, Amsterdam
- Armstrong FA (2002) Voltammetry of proteins. In: Bard AJ, Stratmann M, Wilson GS (eds) Encyclopaedia of electrochemistry, vol 9. Wiley, Weinheim
- Inzelt G (2008) Conducting polymers. A new era in electrochemistry. In: Scholz F (ed) Monographs in electrochemistry. Springer, Berlin
- Kounaves SP, O'Dea JJ, Chandrasekhar P, Osteryoung J (1987) Anal Chem 59:386
- Donten M, Stojek Z, Kublick Z (1984) J Electroanal Chem 763:11
- Wang J, Lu J, Hočevá SB, Farias PAM, Ogorevc B (2000) Anal Chem 72:3218
- Hočevá SB, Svacara I, Ogorevc B, Vytras K (2007) Anal Chem 79:8639
- Scholz F, Schröder U, Gulaboski R (2005) Electrochemistry of immobilized particles and droplets. Springer, Berlin
- Shi C, Anson FC (1998) Anal Chem 70:3114
- Shi C, Anson FC (2001) J Phys Chem B 105:8963

17. Mirčeski V, Komorsky-Lovrić Š, Lovrić M (2007) Square-wave voltammetry. Theory and application. In: Scholz F (ed) Monographs in electrochemistry. Springer, Berlin, p 163
18. Komorsky-Lovrić S, Riedl K, Gulaboski R, Mirčeski V, Scholz F (2002) Langmuir 18:8000
19. Komorsky-Lovrić S, Riedl K, Gulaboski R, Mirčeski V, Scholz F (2003) Langmuir 19:3090
20. Scholz F (2006) Annu Rep Prog Chem C 102:43
21. Quentel F, Mirčeski V, L'Her M (2005) Anal Chem 77:1940
22. Mirčeski V, Quentel F, L'Her M, Elleouet C (2007) J Phys Chem C 111:8283
23. Mirčeski V, Gulaboski R, Scholz F (2004) J Electroanal Chem 566:351
24. Mirčeski V (2004) J Phys Chem B 108:13719
25. Aoki K, Osteryoung J (1988) J Electroanal Chem 240:45
26. de Vries WT (1965) J Electroanal Chem 9:448
27. de Vries WT, van Dalen E (1967) J Electroanal Chem 14:315
28. Aoki K, Tokuda K, Matsuda H (1984) J Electroanal Chem 160:33
29. Aoki K, Tokuda K, Matsuda H (1983) J Electroanal Chem 146:417
30. Shlesinger M (1988) Ann Rev Phys Chem 39:269
31. Weissman M (1988) Rev Mod Phys 60:537
32. Metzler R, Klafter J (2000) Physics Reports 339:1
33. Mirčeski V, Tomovski Ž (2009) J Phys Chem B 113:2794
34. Whittaker ET, Watson GN (1927) A course in modern analysis, vol. 4. Cambridge University Press, Cambridge
35. Erdelyi A, Magnus W, Oberhettinger F, Tricomi FG (1955) Tables of integral transforms, vol. 3. McGraw-Hill, New York
36. Engler H (1997) Differential Integral Equations 10:815
37. Fujita Y (1990) Osaka J Math 27:309
38. Gorenflo R, Luchko Y, Mainardi F (1999) Fract Calc Appl Anal 2:383
39. Mainardi F (1996) Chaos, Solitons and Fractals 7:1461
40. Mainardi F, Pagnini G, Saxena RK (2005) J Comput Appl Math 178:321
41. Mainardi F, Pagnini G (2003) Appl Math Comp 141:51
42. Prüss J (1993) Evolutionary integral equations and applications. Birkhäuser, Basel
43. Podlubny I (1999) Fractional differential equations, mathematics in science and engineering. Academic, New York, 198 pp
44. Schneider WR, Wyss WW (1989) J Math Phys 30:134
45. Wyss W (1986) J Math Phys 27:2782
46. Hilfer R (2000) J Phys Chem B 104:914
47. Nicholson RS, Olmstead ML (1972) Numerical solutions of integral equations. In: Mattson JS, Mark HB, Macdonald HC (eds) Electrochemistry: calculations simulation and instrumentation, vol. 2. Marcel Dekker, New York, p 120
48. Mirčeski V, Tomovski Ž (2008) J Electroanal Chem 619–620:164
49. Mirčeski V, Quentel F, L'Her M, Pondaven A (2005) Electrochim Commun 7:1122
50. Gulaboski R, Mirčeski V, Pereira CM, Cordeiro MNDS, Silva AF, Quentel F, L'Her M, Lovrić M (2006) Langmuir 22:3404